

Ferromagnetism makes a doped semiconductor less shiny

F.P. Mena,¹ J.F. DiTusa,² D. van der Marel,^{1,3} G. Aeppli,⁴
D.P. Young,² C. Presura,¹ A. Damascelli,⁵ and J.A. Mydosh⁶

¹*Materials Science Centre, University of Groningen, 9747 AG Groningen, The Netherlands*

²*Department of Physics and Astronomy, Louisiana State University, Baton Rouge, Louisiana 70803 USA*

³*Departement de Physique de la Matiere Condensee,*

Universite de Geneve, CH-1211 Geneve 4, Switzerland

⁴*London Centre for Nanotechnology and Department of Physics and Astronomy, UCL London WC1E6BT, UK*

⁵*Department of Physics & Astronomy, University of British Columbia, Vancouver, B.C. V6T 1Z1, Canada*

⁶*Kamerling Onnes Laboratory, Leiden University, 2500 RA Leiden, The Netherlands,
and Max-Planck-Institute for Chemical Physics of Solids, D-01187 Dresden, Germany*

(Dated: October 20, 2004)

Magnetic semiconductors have attracted interest because of the question of how a magnetic metal can be derived from a paramagnetic insulator. Here our approach is to carrier dope insulating FeSi and we show that the magnetic half-metal which emerges has unprecedented optical properties, unlike those of other low carrier density magnetic metals. All traces of the semiconducting gap of FeSi are obliterated and the material is unique in being less reflective in the ferromagnetic than in the paramagnetic state, corresponding to larger rather than smaller electron scattering in the ordered phase.

PACS numbers: 78.20.-e, 78.30.-j, 72.25.Dc, 71.27.+a

Future technologies based on the control and state of electron spins rather than charges are commonly referred to as spintronics. Efforts to produce materials for spintronics have mostly focused on thin film III-V semiconductors alloyed with manganese [1]. In (GaMn)As, the most fully characterized of these alloys, Mn substitutes a trivalent Ga ion and acts as a shallow acceptor just above the valence band. The Mn²⁺ impurities have a local moment associated with a high spin (S=5/2) configuration, and are ferromagnetically coupled below the Curie temperature (T_C) by a small number of itinerant hole carriers. In metallic and ferromagnetic (FM) (GaMn)As these doped holes reside in an itinerant Mn-derived impurity band [2] about 0.1 eV above the valence band.

Another route to magnetic semiconductors relies on carrier doping into small gap, strongly correlated insulators. The most celebrated is the monosilicide FeSi, which has been investigated for several decades because it has a large 300 K response to magnetic fields that vanishes as T approaches zero [3, 4, 5]. Together with CoSi and the unusual metal MnSi [6], FeSi belongs to the larger group of transition metal monosilicides, allowing chemical substitutions across the entire series without change in the cubic B-20 crystal structure or the nucleation of second phases [3, 4]. Bulk single crystals can be grown and FeSi can be made metallic and FM, with electrical properties which are unusually sensitive to external magnetic fields, by the substitution of Co to form the silicon-based magnetic half metal [3, 7, 8] Fe_{1-y}Co_ySi, whose calculated density of states is shown in Fig. 1.

Given that optical properties are both of fundamental interest and a key to potential spintronic applications [9], we have measured the optical conductivity $\sigma(\omega)$ of Fe_{1-y}Co_ySi. For clean semiconductors, the low- T $\sigma(\omega)$

is dominated by excitations across a gap (E_g) between valence and conduction bands. Chemical doping adds carriers to the valence, conduction, or impurity bands and yields a $T = 0$ $\sigma(\omega)$ which is very similar to that obtained by warming in the undoped case--the dominant low- ω feature is a Drude peak with weight proportional to the carrier density (n) and width Γ measuring the typical scattering rate for the carriers. If the carriers were magnetically polarized their band would be split into majority and minority spin-bands. Eventually the minority band can move above the Fermi energy (E_F) resulting in a redistribution of all the carriers into the majority band. The outcome is a half metal, of which Fe_{1-y}Co_ySi is an excellent example (Fig. 1), because electrons carrying the majority spin belong to a partially filled, metallic band, while those carrying the minority spin belong to an empty (at $T = 0$) conduction band [10]. To accommodate all of the itinerant electrons E_F shifts upward, decreasing the density of states (DOS) at E_F by a factor of $2^{2/3}$. Naively one might expect this reduction in the DOS to reduce the low- ω $\sigma(\omega)$. However, the optical sum rule states that the integral of $\sigma(\omega)$ over ω measures n , so that conservation of n in the parabolic band leads to conservation of $\sigma(\omega)$ through the phase transition as long as Γ and the effective mass (m^*) of the carriers do not change. This is precisely what occurs for spin polarized metals such as CrO₂ and NiMnSb [11, 12]. Similarly, data for (GaMn)As reveal changes to $\sigma(\omega)$ below T_C due primarily to a reduction of Γ and an associated reduction in m^* [2]. As a result $\sigma(\omega)$ increases below 3000 cm⁻¹ making the appearance more reflective. In addition $\sigma(\omega)$ of (GaMn)As displays a resonance at 2000 cm⁻¹ due to the promotion of electrons from the GaAs valence band to Mn acceptor levels which have been broadened into an

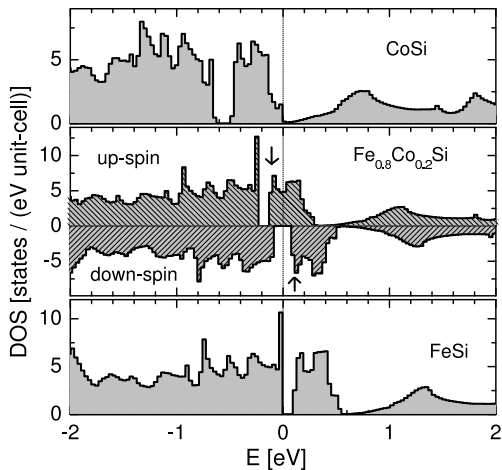


FIG. 1: Calculated DOS. Electronic density of states calculated using the local density approximation (LDA) with the Gunnarsson-Lundquist exchange correlation potential carried out self consistently using the full potential linear muffin-tin orbital method [8]. For $\text{Fe}_{0.8}\text{Co}_{0.2}\text{Si}$ a non-integer charge to iron in FeSi was assigned. Arrows are approximate E_F in unpolarized state.

impurity band [2]. Finally, EuB_6 and $\text{La}_{1-x}\text{Sr}_x\text{MnO}_3$ display the most impressive increases in reflectivity, due to simultaneous ferromagnetic and insulator- to-metal transitions [13, 14].

We used vapor transport, light image furnace floating zone, and modified tri-arc Czochralski methods to grow single crystals from high purity starting materials. X-ray spectra showed all samples to be single phase with a lattice constant linearly dependent on y demonstrating that Co successfully replaces Fe over the entire concentration range ($0 \leq y \leq 1$). Energy dispersive X-ray microanalysis yielded results consistent with the nominal concentrations. Reflectivity ($R(\omega)$) was measured from 30 to 6000 cm^{-1} while ellipsometry gave the dielectric function from 6000 to 36000 cm^{-1} . Between 30 and 6000 cm^{-1} we used Kramers-Kronig (KK) relations, along with a Hagen-Rubens extrapolation of $R(\omega)$ data to $\omega = 0$, to obtain the phase of $R(\omega)$, and subsequently $\epsilon(\omega)$. $\sigma(\omega)$ was found via $\text{Re}\sigma = (\omega/4\pi)\text{Im}\epsilon(\omega)$. We have carefully checked that $\sigma(\omega)$ is not significantly altered by our choice of high- and low- ω terminations. The KK output was locked to the ellipsometrically measured $\epsilon_1(\omega)$ and $\epsilon_2(\omega)$.

Figs. 2 and 3 display $R(\omega)$ and $\sigma(\omega)$ of three crystals for several T 's over a wide ω range. We begin with pure CoSi (top frames in Figs. 2 and 3), long known as a dia-

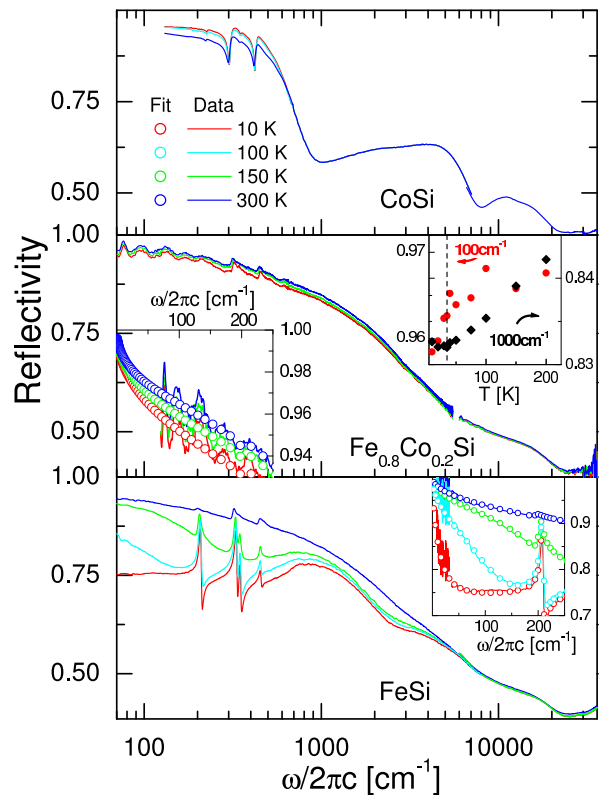


FIG. 2: Near normal $R(\omega)$ of FeSi, CoSi, and $\text{Fe}_{0.8}\text{Co}_{0.2}\text{Si}$. Insets: Expanded view of $R(\omega)$ (solid lines) and fit to $R(\omega)$ at low- ω (open circles). Middle-panel inset: T -dependence of $R(\omega)$ at 100 and 1000 cm^{-1} ; dashed line is T_C .

magnetic metal with a very low carrier density, $\sim 1\%$ of electrons/formula unit [15]. Our data agree with the simple ideas of $\sigma(\omega)$ of a low n metal—there is a small Drude peak centered at $\omega = 0$ which coexists with inter-band transitions beginning at $\sim 1000 \text{ cm}^{-1}$. At 10 K $\Gamma = 165 \text{ cm}^{-1}$, which in the simplest analysis implies a carrier mean free path of 5 nm. The main effect of warming to 300 K is to raise Γ by less than $k_B T$.

The lower frames of Figs. 2 and 3 display data for the alloy's other end member, insulating FeSi. $\sigma(\omega)$ which shows no hint of a band gap at 300 K, is almost completely suppressed below 600 cm^{-1} upon cooling to 10 K, as in Ref. [16] which emphasized that in a conventional band picture, remnants of a 60 meV gap should be clearly visible at 300 K (26 meV) [16, 17]. A second important feature is that the energy range over which $\sigma(\omega)$ changes as T is reduced is extremely large. Estimates based on the data of Fig. 3 agree with previous reports of a lack of spectral weight conservation to energies above 80 times E_g [16]. These two observations represent a miserable failure of the independent electron model for FeSi [18].

Doping FeSi via substitution of Co for Fe yields similar problems for the standard model underlying semi-

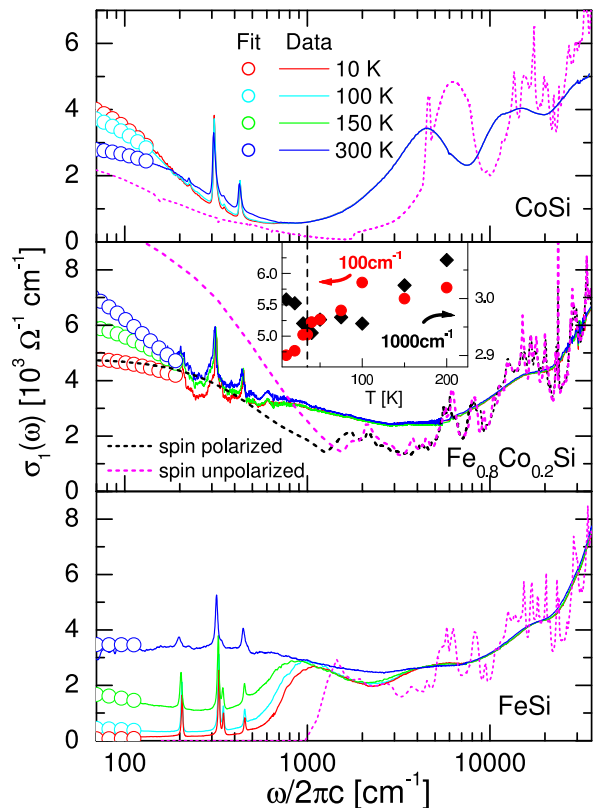


FIG. 3: Real part of $\sigma(\omega)$ of FeSi, CoSi, and $\text{Fe}_{0.8}\text{Co}_{0.2}\text{Si}$. (solid lines and open circles). Dashed lines are $\sigma_1(\omega)$ obtained from the LDA band structure calculations, evaluated [8] with a k -space integration over 216 points in the irreducible part of the Brillouin zone. The calculations fix both the positions of the interband transitions and the weight of Drude peak. Widths (Γ) of the Drude peaks were chosen to minimize deviation from experiment. For $\text{Fe}_{0.8}\text{Co}_{0.2}\text{Si}$, polarized calculation is a much better estimate for Drude weight than unpolarized calculation, even at 300 K, consistent with short range magnetic order well above T_C . Notwithstanding the huge $\Gamma = 600 \text{ cm}^{-1}$ used, substantial spectral weight associated with Co doping is unaccounted for. Inset: T -dependence of $\sigma_1(\omega)$ at 100 and 1000 cm^{-1} ; dashed line is T_C .

conductor optics. In contrast to the data for pure CoSi, but in agreement with our findings for FeSi at 300 K, $\text{Fe}_{0.8}\text{Co}_{0.2}\text{Si}$ displays a $\sigma(\omega)$ which decays weakly from $\omega = 0$ to 3000 cm^{-1} , and all traces of the gap in the pure FeSi parent are obliterated [19]. Even with the assumption of a scattering rate in excess of the 60 meV gap of FeSi, a simple Drude analysis (dashed lines in Fig.3) based on our band structure calculations cannot account for $\sigma(\omega)$. We conclude that treating the electrons in $\text{Fe}_{1-y}\text{Co}_y\text{Si}$ as a simple Fermi liquid formed in the conduction band is incorrect, notwithstanding the remarkable simplicity of aggregate $\omega = 0$ properties such as the normal Hall effect and ordered magnetization, which correspond to one carrier and one polarized spin per Co atom [3].

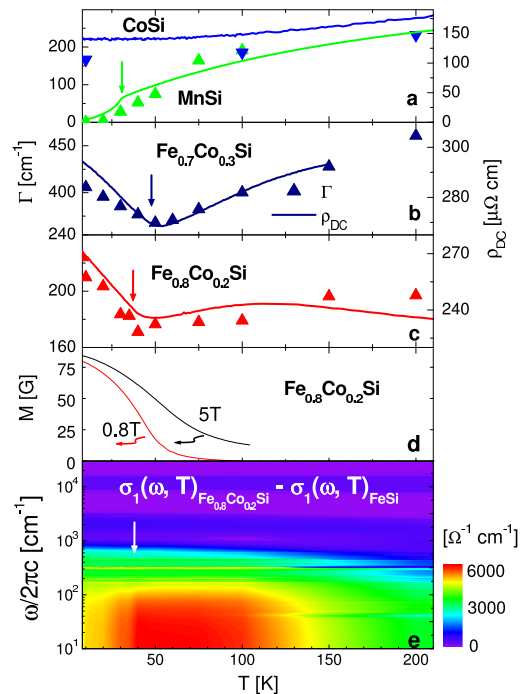


FIG. 4: Low temperature scattering rate (Γ), DC resistivity (ρ), magnetization (M), and optical conductivity ($\sigma(\omega)$). (a), (b), and (c) ρ (solid lines) and Γ (triangles). (d) M . (e) Difference between $\sigma(\omega)$ of $\text{Fe}_{0.8}\text{Co}_{0.2}\text{Si}$ and FeSi as function of ω and T . Data and fit in Fig.3 have been used. At low- ω an additional decrease in $\sigma(\omega)$ can be seen below T_C in $\text{Fe}_{0.8}\text{Co}_{0.2}\text{Si}$. The arrows in parts a, b, c, and e are T_C .

Beyond showing that the parent insulator and its electron-doped derivative violate standard ideas about undoped and doped semiconductors, Figs. 2 and 3 also reveal that $\text{Fe}_{1-y}\text{Co}_y\text{Si}$ defies expectations for itinerant magnets. In particular, cooling yields a loss of spectral weight of a different qualitative nature than seen for FeSi, where it occurs throughout the gapped region. The loss is apparent not only in $\sigma(\omega)$ derived via Kramers-Kronig from the raw data, but also in the directly observed reflectivity. Thus, in contrast to what occurs for all other metallic ferromagnets, including isostructural MnSi [6] and (Ga,Mn)As [2], the approach and onset of magnetic order at $T_C = 36 \text{ K}$ decreases the reflectivity (shininess) of $\text{Fe}_{1-y}\text{Co}_y\text{Si}$.

Fig. 4 and the insets in the middle frames of Figs. 2 and 3 reveal more detail on the evolution of the optical data with T , and allow comparison to transport and magnetization results. The reflectivity (middle frame inset of Fig. 2) at low- ω simply follows the D.C. conductivity, which experiences its main drop below T_C . For higher ω , the reflectivity decreases continuously from 300 K, with no visible anomaly at T_C . The disappearance of anomalies near T_C as ω increases agrees with the extended critical regime, or superparamagnetism (field induced short range order), indicated by the magnetization data of Fig.

4d. Here a modest (compared to $k_B T$) external field of 5 T produces very appreciable polarization to T 's as high as 100 K $\sim 3T_C$. Fig. 4e shows $\sigma(\omega, T)$ of $\text{Fe}_{0.8}\text{Co}_{0.2}\text{Si}$ after subtraction of $\sigma(\omega)$ of FeSi, revealing where the added carriers reside in the excitation spectrum of the nominally pure compound. Cooling builds up the differential (relative to the insulator) spectral weight down to T_C , whereupon there is a loss especially apparent below 200 cm^{-1} . Again, our observation of a reduced spectral weight below T_C contradicts both the standard models based on independent quasiparticles and measurements for other magnetic semiconductors [2].

In addition, cooling below T_C causes the wide Drude-like peak to broaden, rather than to narrow. We have parameterized the low- ω $\sigma(\omega)$ by fitting the standard Drude form, superposed on a T -independent Lorentzian peak at 800 cm^{-1} , to the data. Figs. 4a-c display the resulting Γ 's, which track the bulk resistivities (σ_{DC}^{-1}) and undergo a sharp upturn below T_C . The important and unique contribution of the optical data is to show that the unusual rise in resistivity below T_C is due as much to enhanced scattering as to a reduction in the DOS.

To begin to understand our data, we have derived $\sigma(\omega)$ (Fig. 3) from the band structure (see Fig. 1 and its caption) of $\text{Fe}_{1-y}\text{Co}_y\text{Si}$. The band structure, computed assuming that Co doping only increases the effective charge at the iron site, agrees with the magnetization and Hall effect and more complicated supercell calculations, in that the minority spin Fermi surface resides in a gap [3, 7]. It also supports the idea that Co doping merely adds electrons to rigid bands inherited from the FeSi parent, even revealing, as does experiment, that CoSi (with one extra electron/Fe) is a very low n metal. Another important consequence is that in the polarized state, E_F of the majority spins appears at a DOS minimum, while in the unpolarized state, the DOS at E_F is high. This result is probably responsible for the generally reduced metallicity of $\text{Fe}_{1-y}\text{Co}_y\text{Si}$ as it is cooled.

While band theory (Fig. 1) has some successes, it fails in many significant regards, explaining neither the rapid filling of the gap of FeSi with T , nor the apparent loss of carriers at low- ω , and increase—instead of the conventional decrease—in Γ below T_C of $\text{Fe}_{1-y}\text{Co}_y\text{Si}$. To make progress, the Coulomb interactions need to be considered. How these underpin the moment formation at modest T , as well as the rapid filling of the gap in the parent compound via the paradigm of the Kondo insulator, is discussed elsewhere [18]. The new optical effect in the doped material reported here most likely follows from changes in the effective Coulomb coupling due to quantum mechanical interference of diffusing charge carriers[20]. This feature of disordered metals, hitherto seen only in transport and tunneling, but witnessed optically for the first time in our experiments, induces square-root singularities in the DOS at E_F [20]. Spin-polarization, either from external magnetic fields or a spontaneous magnetization,

shifts the singularities with respect to E_F resulting in a reduction of $\sigma(\omega)$ [20]. Thus $\sigma(\omega)$ and $R(\omega)$ display singular behavior at low T and ω just as we observe. Furthermore, increased Coulomb scattering is apparent in the continuous rise of Γ as T is lowered below T_C .

We have shown that the optical properties of $\text{Fe}_{1-y}\text{Co}_y\text{Si}$ are very different from those for (GaMn)As, even though bulk properties such as the off-diagonal conductivity are remarkably similar[3]. Doping produces an optical response throughout the gap of FeSi, implying that we are dealing not with an impurity band as in (Ga,Mn)As—but rather with carriers donated to the conduction band of FeSi, which cause its gap to collapse. Finally, we have discovered an optical reflectivity which decreases rather increases upon entering the spin-polarized state. The corresponding rise in the scattering rate, uniquely visible in the optical data, demonstrates that the origin of this effect is the Coulomb interaction between electrons in a disordered system.

This work was supported by the US NSF, a Wolfson-Royal Society Award, the Basic Technologies program, the Swiss National Science Foundation through the NCCR 'Materials with Novel Electronic Properties', and the Netherlands—FOM/NWO. We thank A. A. Menovsky and A.I. Poteryaev for assistance with the crystal growth and LDA calculations.

-
- [1] H. Ohno *et al.*, Phys. Rev. Lett. **68**, 2664 (1992); F. Matsukura *et al.*, Phys. Rev. B **57**, R2037 (1998); H. Ohno *et al.*, Appl. Phys. Lett. **69**, 363 (1996); M. L. Reed *et al.*, *ibid.* **79**, 3473 (2001).
 - [2] E. J. Singley *et al.*, Phys. Rev. Lett. **89**, 097203 (2002). E. J. Singley *et al.*, Phys. Rev. B **68**, 165204 (2003).
 - [3] N. Manyala *et al.*, Nature **404**, 581 (2000); N. Manyala *et al.*, Nature Materials **3**, 255 (2004).
 - [4] J. H. Wernick, G. K. Wertheim, and R. C. Sherwood, Mat. Res. Bull. **7**, 1431 (1972); V. Jaccarino *et al.*, Phys. Rev. **160**, 476 (1967).
 - [5] G. Aeppli, Z. Fisk, Comments Condens. Matter Phys. **16**, 155 (1992).
 - [6] F. P. Mena *et al.*, Phys. Rev. B **67**, 241101 (2003); N. Doiron-Leyraud *et al.*, Nature **425**, 595 (2003).
 - [7] J. Guevera *et al.*, Physica B **320**, 388 (2002).
 - [8] F. P. Mena *et al.*, in preparation; O. Gunnarsson, and B. Lundqvist, Phys. Rev. B **13**, 4274 (1976); S. Yu. Savrasov and D. Yu. Savrasov, *ibid.* **46**, 12181 (1992); I. I. Mazin *et al.*, JETP Letters **47**, 113 (1988).
 - [9] S. A. Wolf *et al.*, Science **294**, 1488 (2001).
 - [10] R. A. de Groot *et al.* Phys. Rev. Lett. **50**, 2024 (1983).
 - [11] E. J. Singley *et al.*, Phys. Rev. B **60**, 4126 (1999).
 - [12] F. B. Mancoff *et al.*, Phys. Rev. B **60**, 12565 (1999).
 - [13] L. DeGiorgi *et al.*, Phys. Rev. Lett. **79**, 5134 (1997).
 - [14] Y. Okimoto *et al.*, Phys. Rev. Lett. **75**, 109 (1995).
 - [15] S. Asanabe, D. Shinoda, and Y. Sasaki, Phys. Rev. **134**, 774 (1964).
 - [16] Z. Schlesinger *et al.*, Phys. Rev. Lett. **71**, 1748 (1993).
 - [17] A. Damascelli *et al.*, Phys. Rev. B **55**, 4863 (1997); L.

- DeGiorgi *et al.*, Europhys. Lett. **28**, 341 (1994).
- [18] K. Urasaki and T. Saso, Physica B **281-282**, 313 (2000); M. J. Rozenberg, G. Kotliar, and H. Kajueter, Phys. Rev. B **54**, 8452 (1996); C. Fu, M. P. C. M. Krijn, and S. Doniach, *ibid.* **49**, 2219 (1994).
- [19] M. A. Chernikov *et al.*, Phys. Rev. B **56**, 1366 (1997).
- [20] B. L., Al'tshuler *et al.*, Sov. Sci. Rev. A Phys. **9**, 223 (1987); P. A. Lee, T. V. Ramakrishnan, Rev. Mod. Phys. **57**, 287 (1985).